

Structural tuning of color chromaticity through nonradiative energy transfer by interspacing CdTe nanocrystal monolayers

Neslihan Cicek,¹ Sedat Nizamoglu,¹ Tuncay Ozel,¹ Evren Mutlugun,¹ Durmus Ugur Karatay,¹ Vladimir Lesnyak,² Tobias Otto,² Nikolai Gaponik,² Alexander Eychmüller,² and Hilmi Volkan Demir^{1,a)}

¹Department of Electrical and Electronics Engineering, Department of Physics, Nanotechnology Research Center, Institute of Materials Science and Nanotechnology, Bilkent University, Ankara TR-06800, Turkey

²Physical Chemistry, TU Dresden, Bergstr. 66b, 01062 Dresden, Germany

(Received 20 December 2008; accepted 18 January 2009; published online 9 February 2009)

We proposed and demonstrated architectural tuning of color chromaticity by controlling photoluminescence decay kinetics through nonradiative Förster resonance energy transfer in the heterostructure of layer-by-layer spaced CdTe nanocrystal (NC) solids. We achieved highly sensitive tuning by precisely adjusting the energy transfer efficiency from donor NCs to acceptor NCs via controlling interspacing between them at the nanoscale. By modifying decay lifetimes of donors from 12.05 to 2.96 ns and acceptors from 3.68 to 14.57 ns, we fine-tuned chromaticity coordinates from $(x,y)=(0.575,0.424)$ to $(0.632, 0.367)$. This structural adjustment enabled a postsynthesis color tuning capability, alternative or additive to using the size, shape, and composition of NCs.

© 2009 American Institute of Physics. [DOI: 10.1063/1.3079679]

Precisely tuning shades of color chromaticity is critically important in solid state lighting particularly to achieve application specific spectral illumination (e.g., for indoor applications). For this purpose semiconductor nanocrystals (NCs) have attracted considerable interest with their highly tunable optical properties and have been exploited in various color conversion light emitting diode (LED) applications.¹⁻⁶ Such color tuning of semiconductor quantum dots is enabled by bandgap engineering of the semiconductor crystal, controlling their composition, shape, and size (based on the quantum confinement effect).⁷ However, all of these parameters are commonly controlled and set during the synthesis process. As a postsynthesis alternative to these, we propose and demonstrate the control of nonradiative Förster resonance energy transfer (FRET) in NC emitters in film to conveniently tune their collective color after their synthesis. Locating such NCs in a layered architecture with a gradient of bandgap in a precisely controlled close proximity (<10 nm) of each other enables the control of FRET at a desired level of energy transfer from electronically excited donor NCs (with a wider bandgap) to luminescent acceptor NCs (with a narrower bandgap). Consequently, the controlled level of FRET sets the operating color.

Significant progress in FRET (Ref. 8) related studies on NCs has been achieved in the past decade.⁹⁻¹¹ Because of the sensitive spatial and spectral dependence of FRET, it has been used as nanoscale rulers and light harvesters.¹² In thin film devices, different structures and types of NCs have been investigated to improve the energy transfer by using layer-by-layer (LbL) assembly technique, which allows for the sequential arrangement of multilayered micro- to nanoscale structures of NCs.¹³⁻¹⁵ Franzl *et al.*¹⁶ demonstrated efficient FRET in LbL assembled bilayers of CdTe NCs. In another structure, alternating layers of NCs and polyelectrolytes have been assembled to form a funnel-like bandgap variation

toward the center NC layer for efficient energy harvesting.¹⁷ Also, LbL structures have been constructed by directly attaching oppositely charged NCs without using any linker polymer for further increased energy transfer rates.¹⁸ These previous studies have demonstrated FRET and related dynamics in these engineered LbL NC structures. However, controlling FRET for color tuning of NC emitters has not been investigated or reported to date.

In this letter, we introduce and present the control of photoluminescence (PL) decay kinetics by using nonradiative Förster energy transfer to fine tune the color chromaticity of NC emitters via spatially interspacing them at the nanoscale for LED applications. This architectural adjustment provides a postsynthesis and highly sensitive tuning ability as an alternative to the conventional approaches of controlling the size, shape, and composition of NCs during their synthesis. For that, by modifying decay lifetimes, we tune the color mixing of NC composites that contain LbL assembled donor- and acceptor-NC monolayers (MLs) with polyelectrolyte spacers in a stacked architecture. As a proof-of-concept demonstration, we tuned chromaticity coordinates from the only donor-NC case of $(x,y)=(0.575,0.424)$ to the donor-acceptor NC cases of $(0.581, 0.416)$, $(0.613, 0.385)$, and $(0.632, 0.367)$ using five, three, and one MLs of polyelectrolyte spacing between NCs, respectively (Fig. 1).

We synthesized water-soluble negatively charged CdTe NCs stabilized with thioglycolic acid in accordance with Ref. 19. Two different fractions of these NCs with average particle diameters of 2.9 and 3.7 nm, as estimated from the size curve in Ref. 20, were chosen for their LbL construction. The combination of these two differently sized NC samples presents an energy gradient of 161 meV for nonradiative energy transfer with a Förster radius of 4.6 nm as computed using Eq. (1), where κ^2 is the dipole orientation factor ($2/3$ for random orientation), n is the refractive index of the intermediate medium, Q_D is the quantum yield of the donor, and $J(\lambda)$ is the spectral overlap integral.

$$R_0 = 0.211[\kappa^2 n^{-4} Q_D J(\lambda)]^{(1/6)} (\text{Å}). \quad (1)$$

^{a)}Electronic mail: volkan@bilkent.edu.tr. Tel.: +90(312) 290-1021. FAX: +90(312) 290-1015.

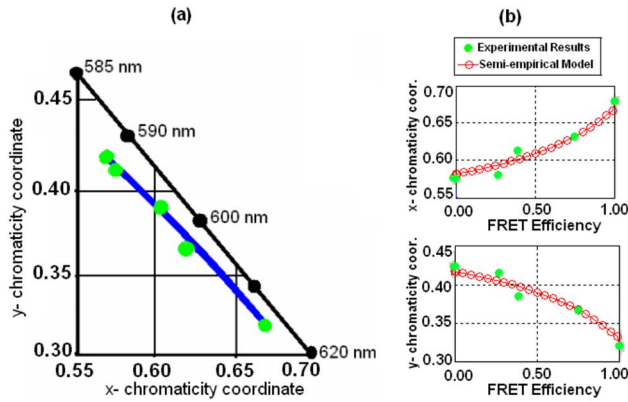


FIG. 1. (Color online) (a) Commission Internationale De L'Eclairage (CIE) chromaticity diagram for the tuning of chromaticity coordinates in our LbL spaced NC samples and (b) their semiempirical analytical model simulation results for color tuning based on FRET efficiency along with the experimental results.

The quantum yield of these CdTe NCs in solution was measured to be 26% (by comparison with rhodamine B) and their quantum yield was 10% in the solid state film (as measured using an integrating sphere). In their LbL assembly, positively charged polymer poly allylamine (PAA) and negatively charged polymer poly styrene sulfonate (PSS) were used as linkers. Their working concentrations were 2 mg ml^{-1} of PSS and 0.5% of PAA, both in 0.1 M NaCl. For the multilayer LbL construction, a computer controlled multivessel dip coater (Nima Technology) was employed. To form a NC ML, the substrate was dipped into an aqueous solution of negatively charged CdTe NCs (with the smaller size of 2.9 nm to serve as donors or with the larger size of 3.7 nm as acceptors), both with a particle concentration of $1.3 \mu\text{M}$ in 0.1 M NaCl for 10 min, and then was rinsed in purified water for 2 min.

To construct polyelectrolyte interspacing of a desired thickness, multiple MLs of PAA and PSS films were consecutively formed in alternating order by dipping in their respective solutions for 10 min and rinsing in water for 2 min and repeating this sequence as many times as required. A similar approach of controlled interspacing was also previously utilized for plasmonic coupling in the work of Kulakovich *et al.*²¹ In our implementation, the heterostructure unit of spacer-NC-spacer-NC was repeated for ten times to complete the entire three-dimensional layered construction of each sample. In the repeating unit between NC MLs, only PAA was used for 1 ML interspacing, then PAA-PSS-PAA for 3 ML interspacing, and finally PAA-PSS-PAA-PSS-PAA for 5 ML interspacing. Since a single polymer ML provides a

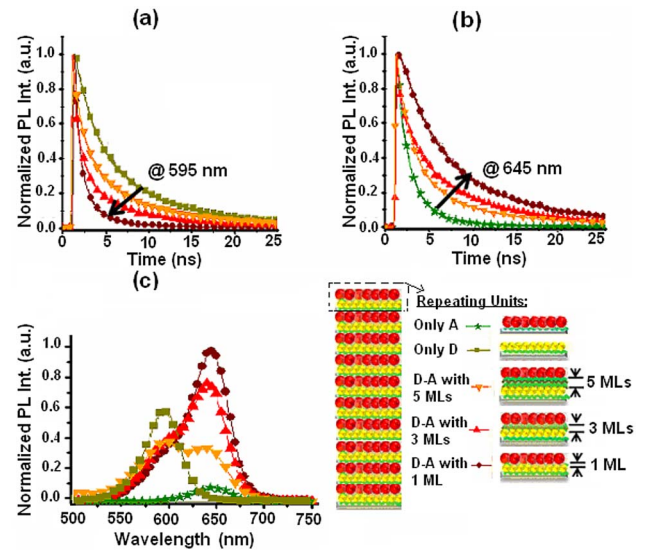


FIG. 2. (Color online) Time-resolved PL decays of small (donor) and large (acceptor) CdTe NCs that are spaced with 1 ML polyelectrolyte=1.0 nm, 3 ML=2.2 nm, and 5 ML=3.4 nm (a) at the donor peak emission wavelength (595 nm) and (b) at the acceptor peak emission wavelength (645 nm) and (c) steady-state PL spectra of donor, acceptor, and controllably spaced donor-acceptor samples.

thickness of $\sim 0.6 \text{ nm}$ and the surface capping of NCs provides $\sim 0.2 \text{ nm}$ according to our atomic force microscopy and ellipsometry measurements, our NC MLs are spaced at $\sim 1.0, 2.2,$ and 3.4 nm apart from each other for 1, 3, and 5 MLs of polyelectrolyte spacing. For our control samples we also fabricated only small (donor) NCs and only large (acceptor) NCs.

We investigate the PL kinetics of our samples with carefully adjusted interspacing between NC MLs using time-resolved PL spectrometer (FluoTime 200, PicoQuant). Figures 2(a) and 2(b) present the PL decays of our only donor, only acceptor, and donor-acceptor samples, separately both at the donor and acceptor peak emission wavelengths of 595 and 645 nm, respectively. In these measurements, FRET from the donor NCs to the acceptor NCs is evident from the simultaneous observations of decreased decay lifetime of the donor NCs and increased decay lifetime of the acceptor NCs. In Figs. 2(a) and 2(b) when the distance between the donor and acceptor MLs is reduced from 5 to 1 ML, the donors start to decay faster because of their energy transfer to the acceptors, which in turn start to decay slower because of their energy feeding from the donors. As a result, the donor average decay lifetime is decreased from 12.05 to 2.96 ns in the presence of acceptors, while the acceptor average decay

TABLE I. Average decay lifetimes, spectrally integrated relative total photon emission (in photon energies), and FRET efficiencies (η_{FRET}) of our LbL spaced donor-acceptor NC samples along with their control groups (only donors and only acceptors).

Interspacing (MLs)	Average decay lifetime (ns)		Total relative emission (eV)		FRET efficiency (η_{FRET})	
	At 595 nm donor emission	At 645 nm acceptor emission	Donors	Acceptors	Using lifetimes	Using PL intensities
5	8.81	8.24	260.11	63.09	0.27	0.32
3	7.41	10.63	219.69	346.02	0.39	0.43
1	2.96	14.57	164.75	447.44	0.75	0.57
Control	12.05	3.68	384.44	59.67

lifetime is increased from 3.68 to 14.57 ns. Table I gives the associated lifetimes of donor NCs and acceptor NCs in all of the samples.

In Fig. 2(c) the PL spectra of our samples are shown along with their corresponding control groups at the excitation wavelength of 350 nm. As the interspacing between NC MLs is shortened, the PL peak of the donor NCs around 595 nm is quenched as a result of transferring their excitation energy, while the PL peak of the acceptor NCs around 645 nm is enhanced owing to their energy transfer feeding. Using Gaussian fits to the steady-state emission of our samples, total photon emission energies (spectral areas integrated under Gaussian emission curves) both for small and large NCs are computed per unit area per unit time, as listed in Table I. The total photon energy of only donor emission quenches from a starting level of 384.44 to 164.75 eV in the presence of acceptors, whereas the only acceptor emission enhances from 59.67 to 447.44 eV in the presence of donors. Also, by using the controlled interspacing between donor NCs and acceptor NCs, we gain control on the extent of recycling trapped excitons. Via energy transfer, in addition to the interband excitons, the excitons that are trapped in the midgap are also transferred, with a fraction of which further contributes to the emission of acceptors.²² For example, for 3 ML interspacing, we obtain an emission enhancement of 27% with respect to the total emission sum of only donors and only acceptors. As we further decrease the interspacing to 1 ML, the emission enhancement improves to 38% because of the enhanced energy transfer for the trapped excitons to the acceptor NCs.

Furthermore, we investigate FRET efficiency to reveal the connection between the control of FRET and the resulting color tuning. In Table I, we compute FRET efficiencies from the time-resolved measurements using Eq. (2) and from relative emission levels of the Gaussian fits to the steady-state measurements using Eq. (3), where τ_{DA} is the donors' fluorescence lifetime in the presence of acceptors, τ_D is the donors' fluorescence lifetime in the absence of acceptors, F_{DA} is the donors' integrated fluorescence intensity in the presence of acceptors, and F_D is the donors' integrated fluorescence intensity in the absence of acceptors. Both sets of these FRET efficiencies exhibit similar behavior over the distance. FRET efficiency is increased, as the interspacing between NC MLs is decreased. This determines the amount of color mixing between the donor NCs and acceptor NCs. As a proof-of-concept demonstration, Fig. 1(a) shows the tuning of color chromaticity across (0.581, 0.416), (0.613, 0.385), and (0.632, 0.367), corresponding to 5, 3, and 1 ML interspacings, respectively, when using donors with (0.575, 0.424) and acceptors with (0.680, 0.321). Thereby, controlled energy transfer allows for the ability to tune the collective color of these NCs by only altering the interspacing between them, despite their fixed size and type. For further analytical analysis, we developed a semiempirical analytical approach to model color mixing based on FRET efficiency. Starting with only the donor and only the acceptor experimental emission curves, this model analytically quenches the donor emission and enhances the acceptor emission in accordance with a given level of FRET efficiency and then computes collective color chromaticity coordinates of these FRET-

modified emission curves. This model led to color tuning curves for the chromaticity coordinates of $x(\eta)$ and $y(\eta)$ as a function of the FRET efficiency η presented in Eq. (4). Figure 1(b) shows that these simulation results are in good agreement with the experimental data, exhibiting consistent trend in color tuning using FRET.

$$\eta_{\text{FRET}} = 1 - \frac{\tau_{DA}}{\tau_D}, \quad (2)$$

$$\eta_{\text{FRET}} = 1 - \frac{F_{DA}}{F_D}, \quad (3)$$

$$x(\eta) = 0.086\eta + 0.573, \quad y(\eta) = -0.085\eta + 0.426. \quad (4)$$

In conclusion, we presented architecturally controlled tuning of PL decay kinetics and color chromaticity for NC-based LbL spaced heterostructures using FRET. These proof-of-concept demonstrations show that controllably spaced NC constructions can be conveniently utilized for precise spectral tuning of color mixing in color conversion LEDs.

This work is supported by ESF-EURYI, TUBA-GEBIP, EU-PHOREMOST-NoE (Grant No. 511616), EU-MC-IRG-MOON (Grant No. 021391), and TUBITAK EEEAG (Grant Nos. 106E020, 104E114, 107E080, 107E297, 105E065, and 105E066).

- ¹M. C. Schlamp, X. Peng, and A. P. Alivisatos, *J. Appl. Phys.* **82**, 5837 (1997).
- ²J. S. Steckel, P. Snee, S. Coe-Sullivan, J. P. Zimmer, J. E. Halpert, P. Anikeeva, L.-A. Kim, V. Bulovic, and M. G. Bawendi, *Angew. Chem., Int. Ed.* **45**, 5796 (2006).
- ³S. Nizamoglu, T. Ozel, E. Sari, and H. V. Demir, *Nanotechnology* **18**, 065709 (2007).
- ⁴S. Nizamoglu and H. V. Demir, *J. Opt. A, Pure Appl. Opt.* **9**, S419 (2007).
- ⁵S. Nizamoglu, G. Zengin, and H. V. Demir, *Appl. Phys. Lett.* **92**, 031102 (2008).
- ⁶U. Banin, *Nat. Photonics* **2**, 209 (2008).
- ⁷S. V. Gaponenko, *Optical Properties of Semiconductor Nanocrystals* (Cambridge University Press, Cambridge, England, 1998).
- ⁸T. Förster, *Ann. Phys.* **437**, 55 (1948).
- ⁹C. R. Kagan, C. B. Murray, and M. G. Bawendi, *Phys. Rev. B* **54**, 8633 (1996).
- ¹⁰J. Sun, M. Gao, M. Zhu, J. Feldmann, and H. Möhwald, *J. Mater. Chem.* **12**, 1775 (2002).
- ¹¹A. A. Mamedov, A. Belov, M. Giersig, N. N. Mamedova, and N. A. Kotov, *J. Am. Chem. Soc.* **123**, 7738 (2001).
- ¹²J. R. Lakowicz, *Principles of Fluorescence Spectroscopy* (Springer, New York, 2006).
- ¹³G. Decher, *Science* **277**, 1232 (1997).
- ¹⁴S. A. Crooker, J. A. Hollingsworth, S. Tretiak, and V. I. Klimov, *Phys. Rev. Lett.* **89**, 186802 (2002).
- ¹⁵A. Shavel, N. Gaponik, and A. Eychmüller, *Eur. J. Inorg. Chem.* **2005**, 3613 (2005).
- ¹⁶T. Franzl, D. S. Koktysh, T. A. Klar, A. L. Rogach, J. Feldmann, and N. Gaponik, *Appl. Phys. Lett.* **84**, 2904 (2004).
- ¹⁷T. Franzl, T. A. Klar, S. Schietinger, A. L. Rogach, and J. Feldmann, *Nano Lett.* **4**, 1599 (2004).
- ¹⁸T. Franzl, A. Shavel, A. L. Rogach, N. Gaponik, T. A. Klar, A. Eychmüller, and J. Feldmann, *Small* **1**, 392 (2005).
- ¹⁹A. Shavel, N. Gaponik, and A. Eychmüller, *J. Phys. Chem. B* **110**, 19280 (2006).
- ²⁰A. L. Rogach, T. Franzl, T. A. Klar, J. Feldmann, N. Gaponik, V. Lesnyak, A. Shavel, A. Eychmüller, Y. P. Rakovich, and J. F. Donegan, *J. Phys. Chem. C* **111**, 14628 (2007).
- ²¹O. Kulakovich, N. Strekal, A. Yaroshevich, S. Maskevich, S. Gaponenko, I. Nabiev, U. Woggon, and M. Artemyev, *Nano Lett.* **2**, 1449 (2002).
- ²²S. Nizamoglu and H. V. Demir, *Opt. Express* **16**, 13961 (2008).